EFFECT OF PLASTICITY AND NORMAL STRESS ON THE UNDRAINED SHEAR MODULUS OF CLAYEY SOILS

MEHRAB JESMANI, HAMED FAGHIHI KASHANI and MEHRAD KAMALZARE

about the authors

Mehrab Jesmani
Imam Khomeini International University,
Department of Civil Engineering
Ghazvin, Iran
E-mail: mehrabjesmani@yahoo.com

Hamed Faghihi Kashani
Imam Khomeini International University,
Department of Civil Engineering
Ghazvin, Iran

Mehrad Kamalzare
Imam Khomeini International University,
Department of Civil Engineering
Ghazvin, Iran
E-mail: mehrad_k@yahoo.com

Abstract

The shear modulus, known as G_{max}, is a key parameter for predicting the static and dynamic behavior of soils. Its value decreases by increasing the shear strain. This is because of reducing the soil's stiffness as a result of increasing the shear deformation. The increasing of the shear modulus by increasing the shear strain is affected by some of the soil properties, such as the Void ratio (e), the Over consolidated ratio (OCR), the Normal stress (σ), the Plasticity index (PI), the Water content (ω%), the Shear strain rate, the Soil structure, and the Loading history, etc. In this paper, undrained, direct shear tests were conducted to study the effect of the plasticity index (PI) and the normal stress (σ) on the shear behavior and the shear modulus of remolded clays. The results show that the normalized shear modulus at a constant strain will generally increase as the σ and PI increase, and the common empirical equations for undisturbed soils at γ = 0~0.1 might be applicable for the disturbed soils too.

keywords

plasticity index, normal stress, shear modulus, disturbed clayey soils

1 INTRODUCTION

The softening of soil under shear stresses indicates a decrease in the shear modulus (G) in terms of its maximum value (G_{max}) in small strain ranges, which depends on several factors, the most important of these are the PI (plasticity index of soil), the *OCR* (the over consolidation ratio), the normal stress (σ), the void ratio (e), the ω% (percent of moisture), the shear strain speed, the structure of the soil and the history of the loading. Several studies have been performed on this subject to determine the value of G from the void ratio (e), the *OCR*, the PI and the normal effective stress in undisturbed soils. Hardin & Black (1968) [1] suggested the use of equation (1) for over consolidated and normally consolidated clay (NC, OC); equation (2) for sands with round grains; and equation (3) for sands with angular grains.

$$G = 625\frac{OCR^K}{0.3+0.7e^2}\sqrt{pa\times\sigma'} \qquad (1)$$

$$G = 6908\frac{(2.17-e)^2}{1+e}\sigma'^{\frac{1}{2}} \qquad (2)$$

$$G = 3230\frac{(2.97-e)^2}{1+e}\sigma'^{\frac{1}{2}} \qquad (3)$$

Where pa is the atmospheric pressure and K is a constant coefficient depending on PI. The laboratory reports presented by Humphries & Wahls (1968) [2] showed that equation (2) is usable for normally consolidated clay with an ordinary sensitivity. The effects of primary and secondary consolidation on the shear modulus of soil were studied by Hardin & Black (1968) [1] and Humphries & Wahls (1968) [2], and it was revealed that the shear modulus increases during the primary and secondary consolidation. The relationship between the shearing modulus and the other parameters was suggested by Hardin & Drenvich (1972) [3] as equation (4) for undrained, over consolidation clay with an ordinary and relatively low sensitivity.

$$G = 3230\frac{(2.97-e)^2}{1+e}(OCR)^K\ \sigma'^{\frac{1}{2}} \qquad (4)$$

where K is the PI-dependent coefficient. These researchers presented a relationship for the maximum shearing module and the actual stress and strain of the soils, according to equation (5), and amended it for the dynamic state as a general equation (Eq. 6) for undisturbed soils.

$$\tau = \frac{OCR^K}{\dfrac{1}{\dfrac{G_{\max+\gamma}}{\tau_{\max}}}} \qquad (5)$$

$$G = \frac{G_{\max}}{(1+\gamma_h)} \qquad (6a)$$

$$\gamma_h = \left(\frac{\gamma}{\gamma_r}\right)\left[1+ae^{-b\left(\frac{\gamma}{\gamma_r}\right)}\right] \qquad (6b)$$

where a and b are constant values depending on the type of soil and the number of cycles of loading and γ_r is the base strain, which is defined as $\gamma_r = \frac{\tau_{\max}}{G_{\max}}$.

Wahls & Marcuson (1972) [4] studied the effects of confining the effective stress on the variation of the maximum shearing modulus and suggested equation (7), based on the void ratio (in the range between 1.5 and 2.5).

$$G = 445\frac{(4.4-e)^2}{1+e}\sigma_c'^{\frac{1}{2}} \qquad (7)$$

where σ_c' shows the effective confining stress. Kokusho et al. (1982) [5] performed some triaxial dynamic tests on the undisturbed samples and presented equation (8) for the normally consolidated clays in the restrictive limits e = 1.5~4 and $\gamma < 10^{-4}$.

$$G = 90\frac{(7.32-e)^2}{1+e}\sigma_c'^{0}\cdot 6 \qquad (8)$$

Richard & Athanaspoulos (1983) [6] studied the effects of the confining pressure of cohesive soils in undrained conditions on the maximum shearing modulus. Based on their observations, it was demonstrated that the lowering of this pressure causes a sudden fall of G_{max}. The percentage of moisture is another important factor that affects G_{max} variations, and researchers such as We et al. (1984) [7], Qian et al. (1991) [8] and Marinho et al. (1995) [9] studied the effect of this parameter on the G_{max} variation and presented the moisturizing limit when the soil reaches its maximum shearing modulus. Studying the effects of PI and *OCR* on the dynamic shearing modulus of saturated soils was performed by Dobry & Vucetic (1991) [10], and it was shown that by increasing PI in a constant strain, the value of G/G_{max} increases. An increase in the shearing strain speed in normally consolidated clay soils causes a decrease in the dynamic, undrained G/G_{max} value. Lanzo et al. (1997) [11] performed some dynamic tests on remolded clay and sand samples and showed that the diminishing diagram of G_{secant}/G_{max} vs. γ shifts upward by increasing the normal stress and the ratio of over consolidation. In other words, in a constant shearing strain, by increasing the normal stress and the ratio of over consolidation, the G_{secant}/G_{max} increases. In the clay and sand samples, the increase in the shearing strain speed increased the secant shearing modulus in the undrained condition. Zhou Yan Guo (2004) [12] made some tests on saturated clay samples and showed that irregularity in the soil structure leads to a decrease in the hardness and the undrained resistance of the soil. A series of dynamic tests on large-grain soils was conducted by Kalinski & Hardin (2005) [13] and showed that the dimensions of the granules are effective in the maximum shearing module. Zhou Yan Gou et al (2005) [14] showed that the effect of the history of dynamic loading is not less than the effect of the history of non-dynamic loading in saturated sands in undrained conditions. Romo & Ovando (2006) [15] presented a relation that showed that the frame of the apparatus subject to the test could be effective in calculating G_{max}. Bergado et al. (2006) [16] presented the case history of a laboratory evaluation of the interface shear-strength properties of various interfaces encountered in a modern-day landfill with the emphasis on a proper simulation of the field conditions and the subsequent use of these results in a stability analyses of a linear system. Li (2007) [17] implemented the nonlinear shear strength criteria of a power-law type in a finite-element slope-stability analysis. Guetif et al. (2007) [18] proposed a method for evaluating an improvement of the Young's modulus of the soft clay in which a vibrocompacted stone column is installed. From the numerical results the degree of improvement of the Young's modulus of the soft clay was estimated. Also, the zone of influence of the improved soft clay was predicted. Basudhar et al. (2007) [19] made an experimental study on the circular footings resting on a semi-infinite layer of sand that was reinforced with geotextiles. The study highlighted the effect of the footing size, the number of reinforcing layers, the reinforcement placement pattern and the bond length, and the relative density of the soil on the load-settlement characteristics of the footings. Sabermahani et al. (2009) [20] conducted a series of 1-g shaking-table tests on 1-m-high reinforced-soil wall models. The distribution of the shear-stiffness modulus (G) and the damping ratio (D) of the reinforced soil along the wall height were assessed.

Most studies performed by other researchers discussed the effects of other parameters on the shearing modulus or cover the effects of PI and σ on undisturbed samples and in dynamic conditions; therefore, for studying the effects of PI and the normal stress on the static shearing behavior of undisturbed clay and studying the reliability of the existing equations on undisturbed clay soils, in this paper, the results of laboratory tests performed on samples with different values of PI and various normal stresses have been presented. An admissible calibration has been established between the dynamic equations and the results of the static test. In fact, the main purpose of this research is to make a calibration between the dynamic equations and the dynamic tests results of previous investigations, and the results of static tests that have been performed in this study. However, the results of this investigation can be used in different scopes of geotechnical engineering and in various soil structures, such as embankment dams that contain solid structures. For example, a concrete culvert, where plastic clay has been used at the interface of the concrete and the soil; or in water-isolating trenches with plastic clay.

2 PROPERTIES OF SAMPLES AND INITIAL TESTS

A soil that indicates the specifications of clay soils used in the practical project was used as the base soil. For making samples with different values of PI, the base clay soil was mixed with different percentages of bentonite and after passing it through a sieve number 40, some tests were performed on samples in order to determine the relative density (G_s), the hydrometer granulation, the Atterberg limits (LL, liquid limit, PL, plastic limit and PI, plasticity index) and the modified compaction of soil in accordance with ASTM standard. The weight percentages of bentonite along with the identifying tests are listed in Table 1 and a diagram of the hydrometer granulation is shown in Fig. 1. It should be noted that the percentage of the bentonite inserted in Table 1 shows the weight percentage of the bentonite used relative to the final weight of the reconstructed samples.

3 PROCESS OF LABORATORY RESEARCHES TO STUDY THE SHEARING PROPERTIES

In this section, the method of making samples and the stages of direct shear tests are introduced. Each one of the remolded samples with different values of PI was compacted in the direct shear apparatus with 95% of dry density and with the optimum moisture in different layers according to the ASTM D-3080 standard and was immersed in water to become saturated. After saturation, the samples were loaded to remove any swelling and the samples returned to their initial dimensions (the amounts of stresses that remove the swelling are shown in Table 2). After the obviation of the swelling, normal loading was made on the three frames made of different values of PI and were immediately sheared in the direct shear apparatus at high speed. The validity of the direct shear test on saturated clay has been presented in different texts (Bowles, 1968 [21] and 1984 [22], Murthy, 1977 [23], Punmia et al. 2005 [24]). In order to determine

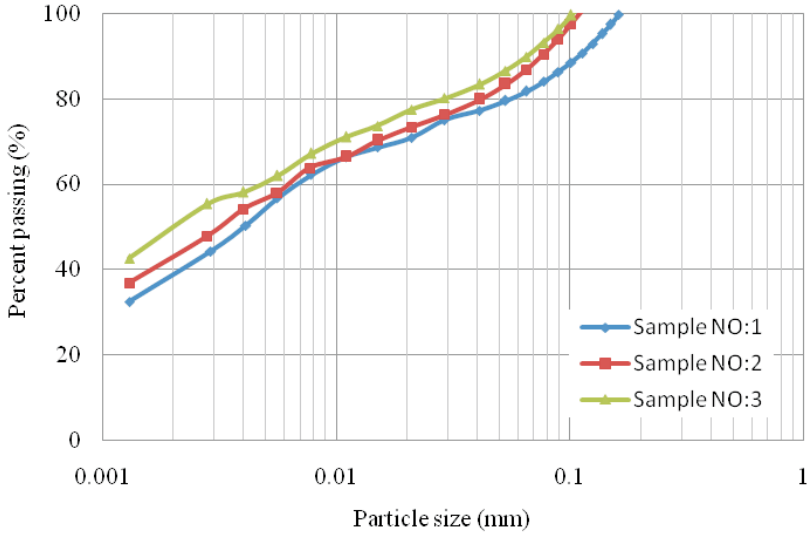

Figure 1. Hydrometer grain-size distribution test results of reconstructed samples.

the rate of load growth, the R_σ coefficient is defined in equation 9.

$$R_\sigma = \frac{\text{Normal stress in direct shear test}}{\text{Stress that removes swelling}} \qquad (9)$$

Table 1. Result of identifying test.

Result	Sample 1	Sample 2	Sample 3
Bentonite Percentage	0	10	20
Soil Type	CL	CL	CL
Liquid Limit (LL)	28	36	43
Plastic Limit (PL)	17	19	20
Plastic Index (PI)	11	17	23
G_s	2.65	2.63	2.60
ω_{opt} (%)	15.0	13.7	12.6
γ_{dmax} (kN/m^3)	18.42	19.13	20.24

The ratio of the increase in load for three frames of each sample is considered to have constant values equal to 1.44, 2.88 and 4.32. The saturation moisture and the amount of stress for removing the swelling is shown in Table 2 and the normal stress for different R_σ (different samples) is specified in Table 3.

Table 2. The saturation moisture and the stress for removing the swelling in the direct shear tests.

Sample	Saturation moisture (%)	Stress for removing swelling (kN/m^2)
Sample 1	19.9	136.3
Sample 2	22.4	272.6
Sample 3	24.8	354.0

Table 3. Normal stress for different R_σ.

Sample	Normal Stress (kN/m^2) (R_σ = 1.44)	Normal Stress (kN/ m^2) (R_σ = 2.88)	Normal Stress (kN/ m^2) (R_σ = 4.32)
Sample 1	196.13	392.26	588.40
Sample 2	392.26	784.53	1176.80
Sample 3	509.94	1019.89	1529.84

4 RESULTS AND DISCUSSION

The results obtained from the samples' identification index tests and the engineering tests analysis as explained before will be discussed in this section.

4.1 RESULTS OF THE IDENTIFICATION INDEX TESTS

In this section, in order to obtain more suitable and accurate results, the values obtained from the testing on samples with 30% and 40% bentonite are presented too.

4.1.1 Effects of the percentage of bentonite on the Atterberg Limits of the samples

As observed in Fig. 2, by increasing the percentage of bentonite in the samples, the Atterberg limits (LL, PL, and PI) are increased. Based on the obtained results, the relationship of the Atterberg limit and the percentage of bentonite of the samples is a relatively linear relation and the rate of increase in the liquid limit with an increase in

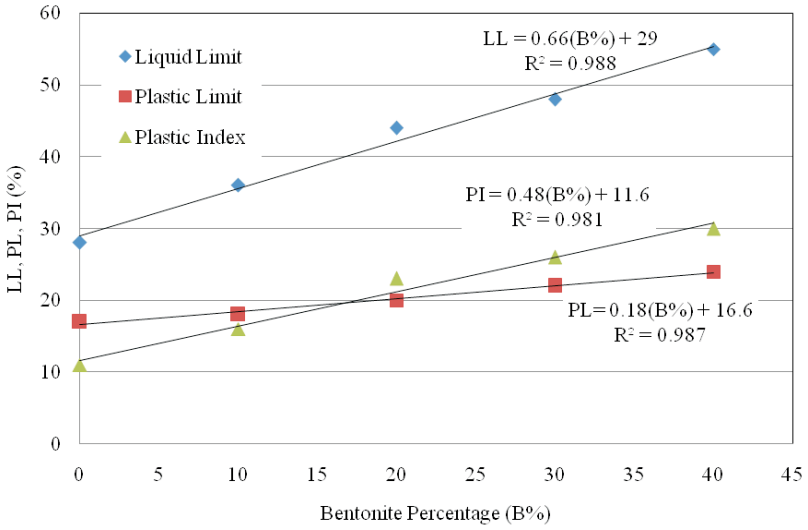

Figure 2. Atterberg limits versus percentage of bentonite.

the percentage of the bentonite of samples exceeds the rate of increase in the plastic index and the plastic limits. The relations obtained based on a linear interpolation among the values of the Atterberg limit and the percentage of bentonite are shown in Fig. 2.

It should be noted that a 10% increase in the amount of bentonite of the samples will cause an increase of 6.45, 1.69 and 4.76 in the liquid limit, the plastic limit and the plasticity index, respectively.

4.1.2 Effect of PI on the optimum and saturation moisture

Based on the obtained results, the increase in the PI of the samples causes an increase in the percentage of the optimum and saturation moisture. It can be seen in Fig. 3 that the process of the increase in the optimum and saturation moistures vs. increase in the PI value follows linear relations and for each 10 percent increase in the PI, the optimum moisture increases 2.51% and saturation moisture increases 4%, on average. The linear formula between the optimum and saturation moisture, and the percentage of bentonite is shown in Fig. 3.

4.1.3 Effects of PI on the maximum dry density

Based on the results of the modified compaction tests, an increase in the values of PI in the samples caused a decrease in the maximum dry density. As can be seen in Fig. 4, the variation of the parameters is almost linear, and for each 10% increase of PI, the maximum dry density decreases by 1.12 kN/m^2.

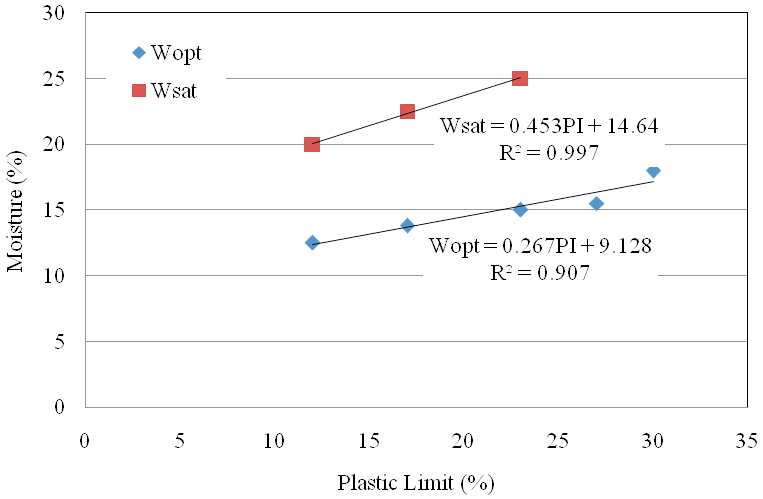

Figure 3. Optimum and saturated moisture versus different percentage of PI.

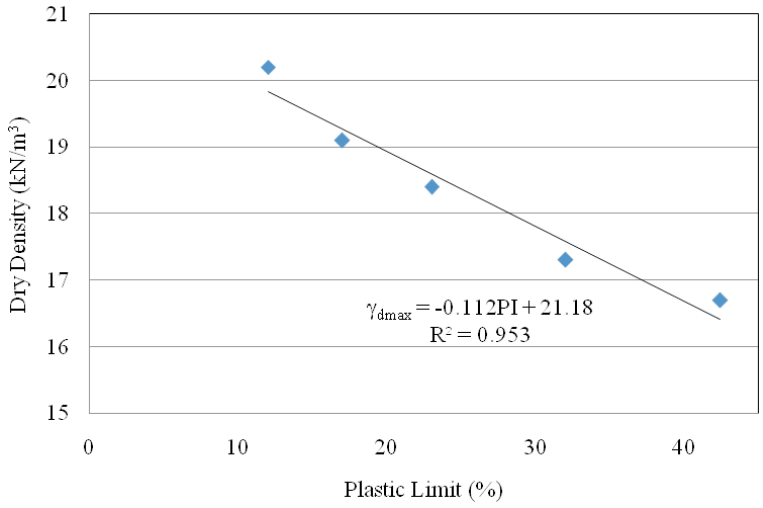

Figure 4. Dry density versus different percentage of PI.

4.2 OBTAINED RESULTS FROM DIRECT SHEAR TESTS

4.2.1 Effects of PI on shearing resistance parameters

Fig. 5 shows the effect of PI on the shear strength parameter. As is clear, an increase in the values of PI leads to an increase of the cohesion and a decrease of the internal friction angle. The relationship between the percentage of bentonite and the cohesion and internal friction angle reveals that for each 10% increase in the amount of bentonite of samples, the cohesion increases 40 kN/m^2 and the internal friction angle decreases by 9.30 degree. The increase in the cohesion and the decrease in the internal friction angle might be attributed to the increase in the clay minerals and the placement of bentonite particles among the large granules of soil.

4.2.2 Effects of R_σ on the variation of the G/G_{max} versus γ

The variation of the normalized shear module (G/G_{max}) vs. the values of the shear strain (γ) for different R_σ is shown in Fig. 6. It can be seen that with an increase in the amount of shear strain (γ), the normalized shearing module (G/G_{max}) decreases. On the other hand, in a constant shear strain as R_σ increases, there is an increase in the amount of G/G_{max}. In Fig. 6(a) the difference between the variations of G/G_{max} in a constant shear strain for different R_σ is shown. A comparison between these two values shows that as the normal stress increases, the change in the amount of G/G_{max} in a constant strain decreases, and this process continues until the failure point is reached.

4.2.3 Effects of PI on variation of G/G_{max} versus γ

The variation of the normalized shearing module (G/G_{max}) vs. the shear strain values (γ) for different values of PI is shown in Fig. 7. As is clear, in a constant R_σ and a constant shear strain, the samples with bentonite showed less G/G_{max} than the samples without bentonite (which has been referred to as base soil). The reason for this could be because of the imbalance made in the soil structure and placement of bentonite among its particles. In addition, a comparison between samples 2, 3 (mixed with bentonite), shows an increasing process of G/G_{max} as a result of the increase in the value of PI at a constant shearing strain.

4.2.4 Variation of G_{max} versus PI and R_σ

Fig. 8(a) and (b) show the relationship between G_{max} and PI and R_σ, respectively. As is clear, with an increase in PI, the G_{max} increases and the effects of R_σ on the process of this increase in such a way that in constant PI the increase in R_σ increases G_{max} (the hardness of soil). The variation of G_{max} vs. PI and R_σ is shown in a 3D contour (Fig. 9).

4.2.5 Verification of the Test Result

In order to determine the efficiency of the existing reliable relations on disturbed soils and comparing the variation of the G/G_{max} versus γ resulting from these relations, and the laboratory results, a new parameter (Δ) is defined as below:

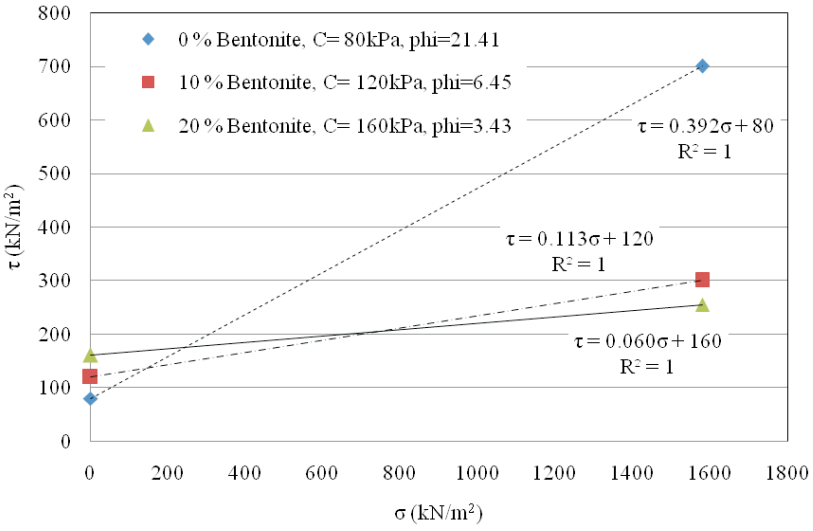

Figure 5. Effect of PI on the shear-strength parameter.

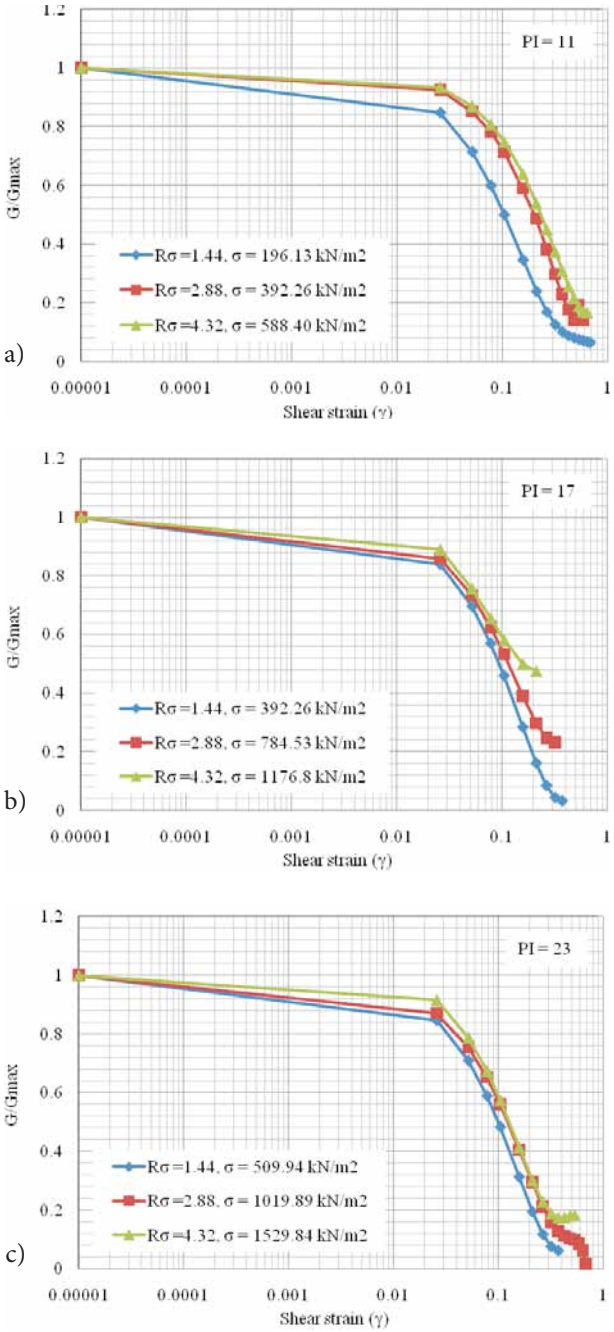

Figure 6. Variation of normalized shear module versus shear strain for different R_σ, (a). PI=11, (b). PI=17, (c). PI=23.

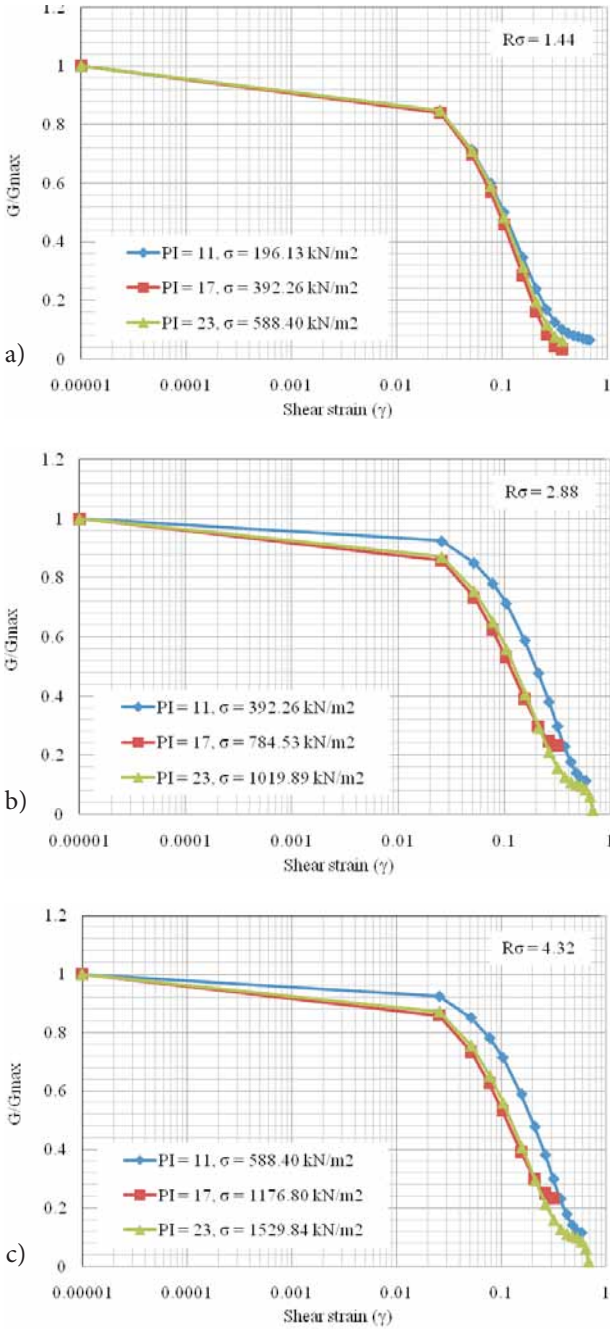

Figure 7. Variation of normalized shear module versus shear strain for different PI, (a). R_σ=1.44, (b). R_σ=2.88, (c). R_σ=4.32.

$$\%\Delta = \left| \frac{\dfrac{G}{G_{\max(Eq)}} - \dfrac{G}{G_{\max(lab)}}}{\dfrac{G}{G_{\max(Eq)}}} \right| \times 100 \qquad (10)$$

It should be noted that the Hardin and Drnevich (1972) [3] equations (Eq. 5, 6), which are known as reliable equations, were used in this comparison. In Fig. 10 to 13, the variation of Δ versus γ for different values of R_σ and PI are shown. With respect to these figures, for strains in the range 0~0.1, the Δ has relatively small values that show the reliability of the presented methods of this study for disturbed soils in small shear strains (less than 0.1); however, in higher shear strains (more than 0.1) the value of Δ increases rapidly.

4.2.6 Effect of R_σ on the variation of Δ versus γ

The increase of R_σ (which leads to an increase in the normal stress) for constant PI, leads to a rapid growth in the value of Δ, which begins from greater strains. This shows the greater compatibility of the Hardin and Drnevich (1972) [3] relations with the lab tests for an increase in the normal stress (Fig. 10 and 11).

4.2.7 Effect of PI on the variation of Δ versus γ

As was shown in Fig. 12 and 13, in sample 1 with no bentonite addition, the value of Δ begins to grow at larger shearing strains than the two other samples (bentonite containing). The process of these changes could be attributed to the lack of bentonite particles among the base soil particles, the maintenance of the initial structure of the soil and subsequently, greater compatibility between its behavior with the Hardin and Drnevich (1972) [3] relations. A comparison between samples 2 and 3 in Fig. 12 and 13 shows that with an increase in the values of PI, the size of Δ starts the rapid increase from the larger strains, which is a proof of the good compatibility between the Hardin and Drnevich (1972) [3] equations and the laboratory tests results.

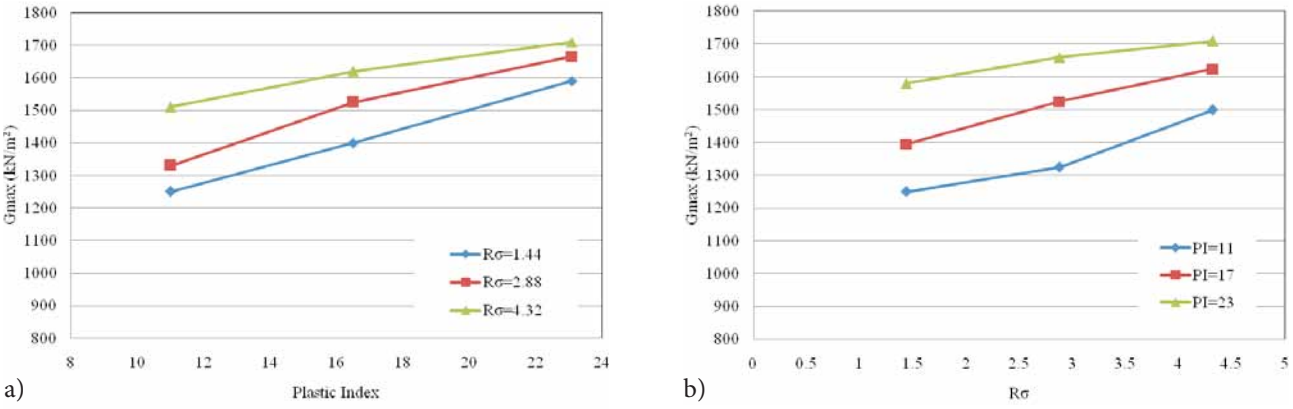

Figure 8. Relationship between G_{max} and PI (a) and R_σ (b).

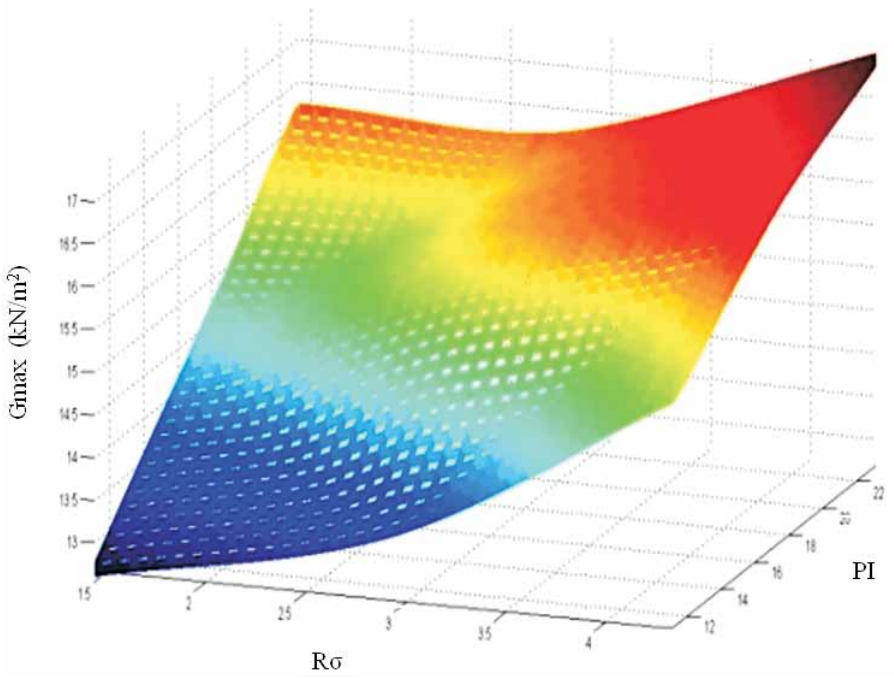

Figure 9. Variation of G_{max} versus PI and R_σ.

5 MATHEMATICAL FORMULATIONS

From the previous sections it can be seen that the plasticity index and the normal stress are the most effective parameters for G_{max}. In this section, one- and two-variables functions are introduced to formulate the G_{max}. Equations 11 and 12 are single-variable functions that show the relationship between G_{max}, PI and σ. These functions are valid for the following values of σ (kN/m^2) and PI: $196 < \sigma < 1530$ and $11 < PI < 23$.

$$G_{max} = -0.674PI^2 + 47.84PI + 908.5 \qquad (11)$$

$$G_{max} = 0.322\sigma + 1272 \qquad (12)$$

The tests results and the trend curves are shown in Fig. 14 and 15.

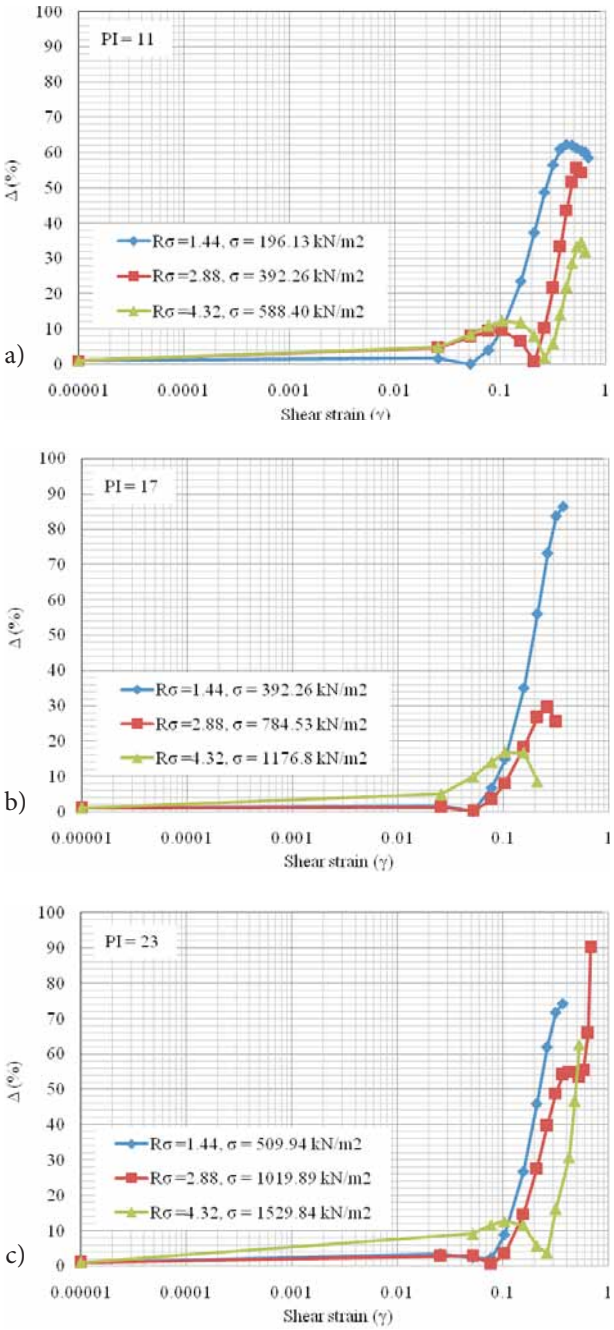

Figure 10. Variation of Δ versus γ for different R_σ (equation 5), (a): PI= 11, (b): PI= 17, (c): PI= 23.

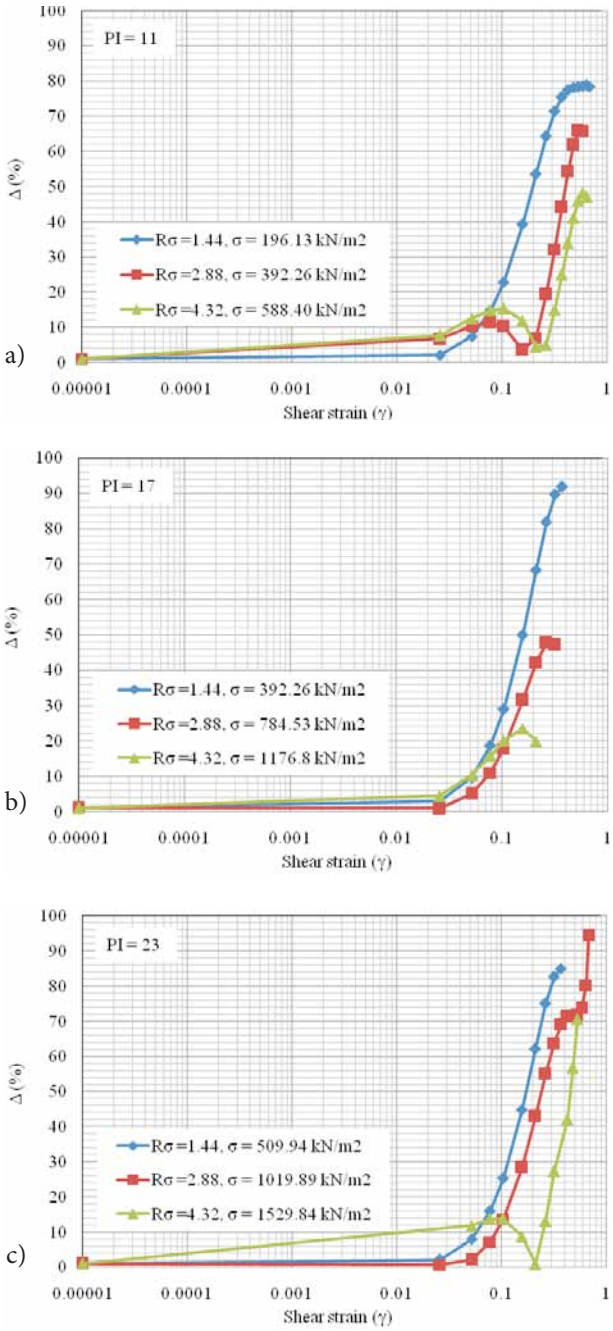

Figure 11. Variation of Δ versus γ for different R_σ (equation 6), (a): PI= 11, (b): PI= 17, (c): PI= 23.

In order to generalize, a two-variables function was also introduced to show the influence of both σ and PI on G_{max} (Eq. 13). The variation of G_{max} versus σ and PI has been shown in Fig. 16.

$$G_{max} = 0.005\sigma^2 + \left(0.02\mathrm{PI}^2 + 0.751\mathrm{PI} - 6.389\right)\sigma + \\ + 5.138\mathrm{PI}^2 - 160.5\mathrm{PI} + 2444 \qquad (16)$$

6 CONCLUSION

The following specific conclusions can be drawn from the study:

- An increase in the percentage of bentonite in the soil causes a significant increase in LL and PI, while this increase has trivial effects on the quantity of PL. It can be seen that for each 10% increase of bentonite

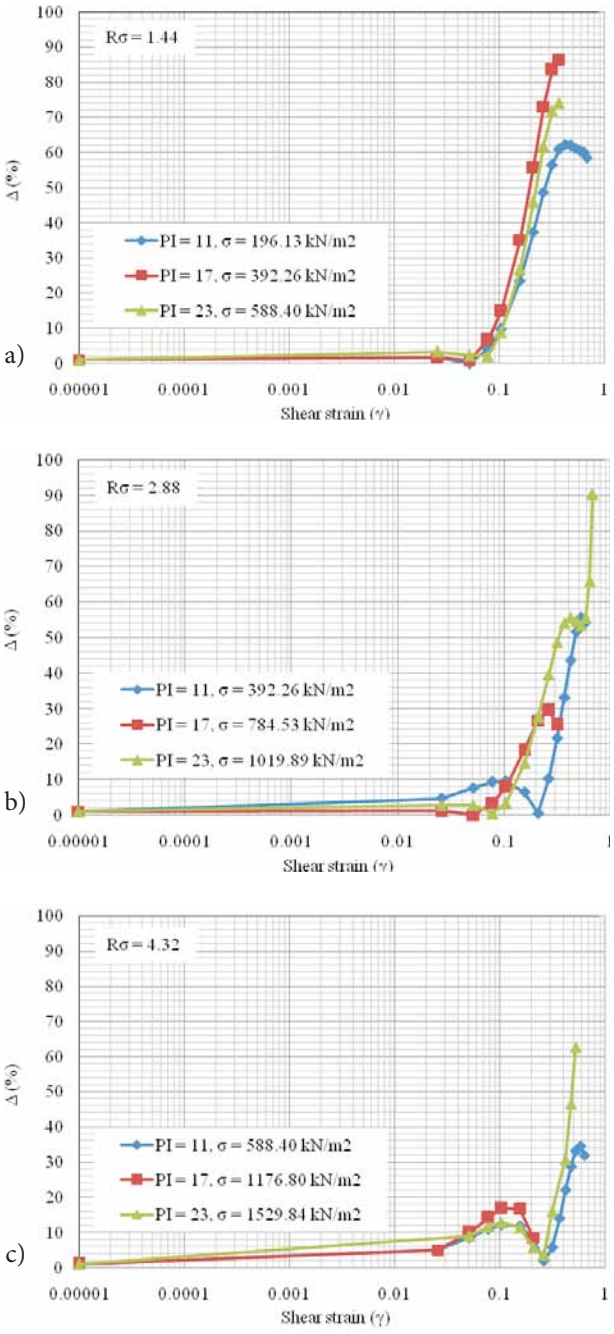

Figure 12. Variation of Δ versus γ for different PI (equation 5) (a): R_σ = 1.44, (b): R_σ = 2.88, (c): R_σ = 4.32.

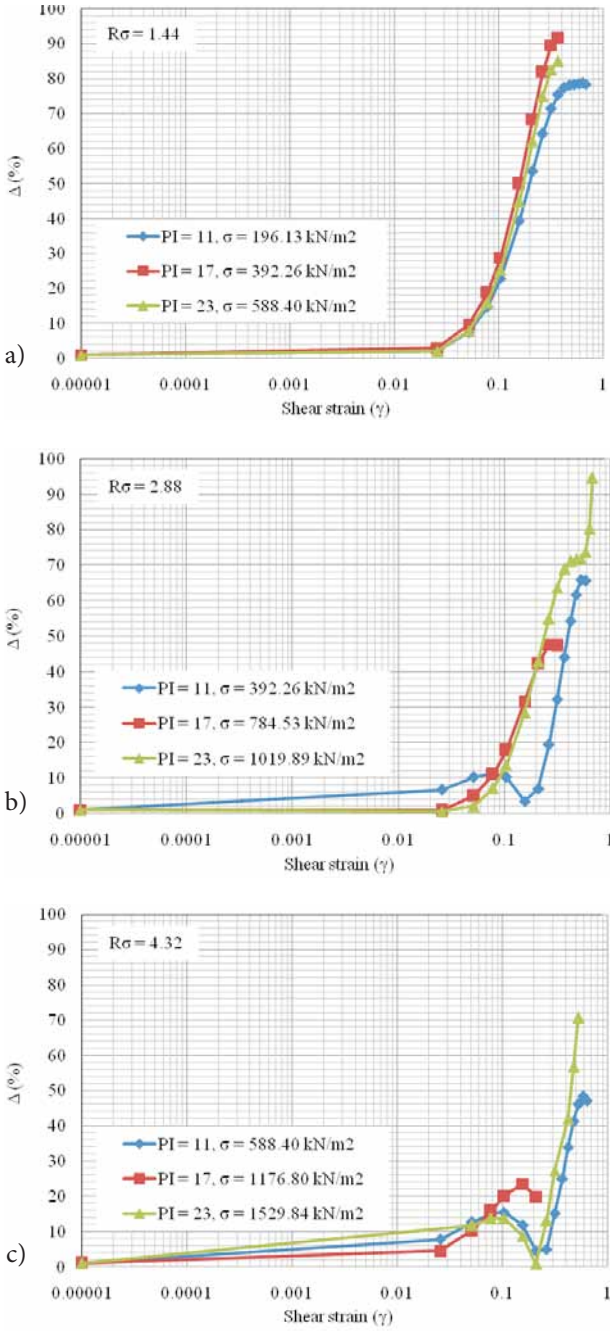

Figure 13. Variation of Δ versus γ for different PI (equation 6) (a): R_σ = 1.44, (b): R_σ = 2.88, (c): R_σ = 4.32.

in the soil samples, LL, PI and PL increase by 6.45%, 4.76% and 1.69% respectively.
- A 10% increase in PI leads to 4% and 2.51% increases in ω_{sat} and ω_{opt} , respectively, and a 1.12kN/m^2 decrease in γ_{dmax}.
- Adding bentonite to the base soil increases the cohesion and decreases the equivalent friction angle by as much as for each 10% increase in bentonite, which causes a 4.76 percent increase in PI, cohesion increases of 40 kN/rn^2 and the internal friction angle decreases by 9.30 degrees.
- The diagram of G/G_{max} vs. γ shifts upward as R_σ increases and in each stage of the R_σ increment (increase in normal stress), the shift of the curve becomes smaller. This increase continues until the soil reaches its highest hardness and is failed due to an increase in the normal stress.
- The G/G_{max} has a higher value in the bentonite-free

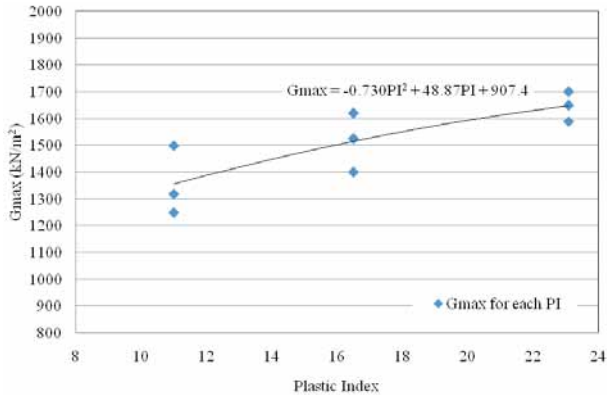

Figure 14. G_{max} versus PI for disturbed soil.

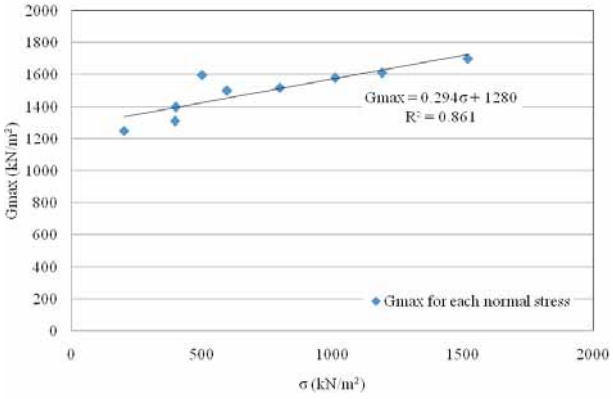

Figure 15. G_{max} versus σ for disturbed soil.

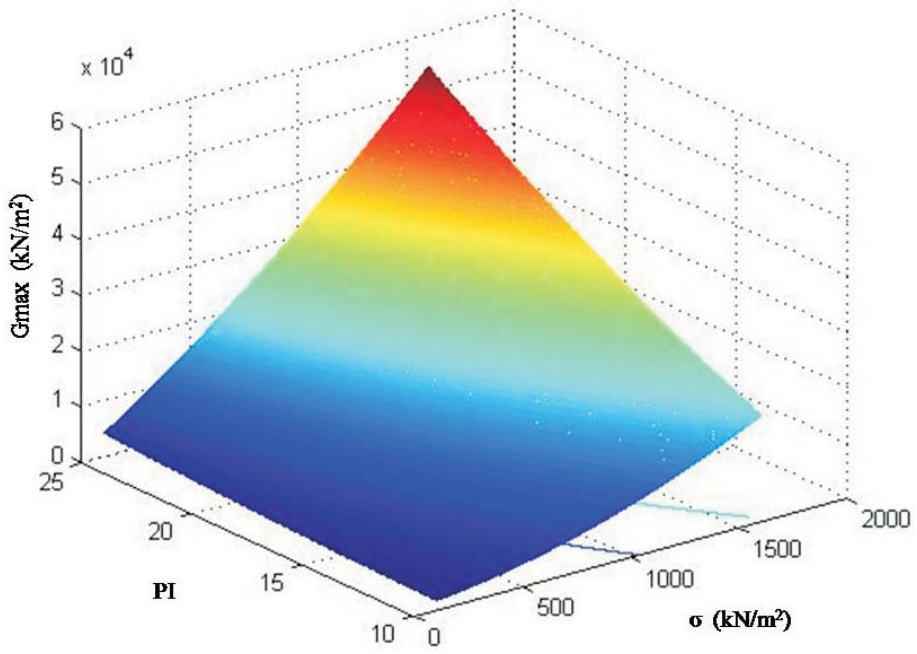

Figure 16. Variation of G_{max} versus σ and PI.

samples than in the bentonite-containing samples for a constant γ.
- In a constant PI, the increase in R_σ causes an increase in G_{max}, and in a constant R_σ, the increase in PI causes an increase in G_{max}.
- The Hardin and Drnevich (1972) [3] equations for undisturbed soils are valid for disturbed soils with shearing strains of less than 0.1.
- In a sample with constant PI, for an increase in R_σ, and, in a sample with constant Rσ as for increase in PI, the coordination between the results from Hardin and Drnevich (1972) [3] and the tests results on disturbed soils increases in strains higher than 0.1. As a result, the shearing strain equal to 0.1 could be considered as a border for the reliability of the Hardin and Drnevich (1972) [3] equation in disturbed soils.

REFERENCES

[1] Hardin, B.O. and Black, W.L. (1968). Vibration Modulus of Normally Consolidated Clay, Journal of the Soil mechanics and Foundation Division, ASCE, 95(2), 353 – 369.

[2] Humphries, F.V. and Wahls, H.E. (1968). Stress Effects on Dynamic Modulus of Clay. Journal of the Soil Mechanics and Foundation Division, ASCE, 94(2), 371– 389.

[3] Hardin, B.O. and Drnevich, V.P. (1972). Shear Modulus and Damping in Soils: Design Equation and Curves. Journal of the Soil Mechanics and Foundation Division, ASCE, 98(7), 667– 692.

[4] Marcuson, W.F. and Wahls, H.E. (1972). Time Effects on on Dynamic Shear Modulus of Clays. Proceeding of ASCE, 98(12), 1359– 1373.

[5] Kokusho, T.A., Yoshidah, Y.A., and Esashi, Y.A. (1982). Dynamic Properties of Soft Clay for Wide Strain Range. Journal of the Soil Mechanics and Foundation Engineering, ASCE, 22(4), 1-18.

[6] Athanasopoulos, G.A. and Richart, F.E. (1983). Effect of Stress Release on Shear Modulus of Clays. Journal of Geotechnical Engineering, ASCE, 109(10), 1233-1245.

[7] Wu, S., Gray D.H. and Richart F.E. (1984). Capillary Effects on Dynamic Modulus of Sands and Silts. Journal of Geotechnical Engineering, ASCE, 110(9), 1188-1203.

[8] Qian, X., Gray, D.H., and Woods R.D. (1991). Resonant Coloumn Tests on Partially Saturated Sands. Geotechnical Testing Journal, ASCE, 14(3), 266-275.

[9] Marinho, E.A.M., Chandler, R.J., and Crilly, M.S. (1995). Stiffness Measurements on an Unsaturated High Plasticity Clay Using Bender Elements. Proceeding of the 1st International Conference on Unsaturated Soils, Paris, Vol. 1, 535-539.

[10] Vucetic, M.L. and Dobry, R.I. (1991). Effect of Soil Plasticity on Cyclic Response. Journal of Geotechnical Engineering, ASCE, 117(1), 89-107.

[11] Lanzo, G., Vucetic, M., and Doroudian M. (1997). Reduction of Shear Modulus at Small Strains in Simple Shear. Journal of Geotechnical Geoenvironmental Engineering, ASCE, 123(11), 1035-1042.

[12] Zhou, Y.G., Chen, Y.M, and Huang, B. (2005). Experimental Study of Seisemic Cyclic Loading Effects on Small Shear Modulus of Saturated Sands. Journal of Zhejiang University SCIENCE, 6 A (3), 229-236.

[13] Hardin, B.O. and Kalinski, M.E. (2005). Estimating the Shear Modulus of Gravelly Soils. Journal of Geotechnical and Geoenvironmental Engineering , ASCE, 131(7), 867-875.

[14] Zhou, Y.G. and Chen, Y.M. (2005). Influence of Seismic Cyclic Loading History on Small Strain Shear Modulus of Saturated Sands. Journal of Soil Dynamic and Earthquake Engineering, 25, 341-353.

[15] Romo, M.P. and Ovando, E. (2006). Modeling the Dynamic Behavior of Mexican Clays. Proceeding 11th World Conference on Earthquake Engineering, Apapulco, Mexico, paper no. 1028.

[16] Bergado, D.T., Ramana, G.V., Sia, H.I., and Varun. (2006). Evaluation of interface shear strength of composite liner system and stability analysis for a landfill lining system in Thailand. Geotextiles and Geomembranes, 24, 6, 371-393.

[17] Li, X. (2007). Finite element analysis of slope stability using a nonlinear failure criterion. Computers and Geotechnics, 34, 3, 127-136.

[18] Guetif, Z., Bouassida, M., and Debats, J.M. (2007). Improved soft clay characteristics due to stone column installation. Computers and Geotechnics, 34, 2, 104-111.

[19] Basudhar, P.K., Santanu Saha, and Kousik Deb. (2007). Circular footings resting on geotextile-reinforced sand bed. Geotextiles and Geomembranes, 25, 6, 377-384.

[20] Sabermahani, M., Ghalandarzadeh, A., and Fakher, A. (2009). Experimental study on seismic deformation modes of reinforced-soil walls. Geotextiles and Geomembranes, 27, 2, 121-136.

[21] Bowles, J. E. (1968). Foundations analysis and design.

[22] Bowles, J. E. (1984). Physical and geotechnical properties of soil. 2nd.ed. McGraw-Hill.

[23] Murthy, V. N. S. (1977). Soil mechanics and foundation engineering. 2nd.ed. Dhanpat Rai.
[24] Punmia, B. C., Ashok Kumar Jain, and Arun Kumar Jain (2005). Soil mechanics and foundations. 16th.ed. New Delhi: Laxmi Publications.